# Electronic Supplementary Information

# Oxidative Addition of Verdazyl Halogenides to $Pd(PPh_3)_4$

Pavel V. Petunin,[ab] Darya E. Votkina,[a] Marina E. Trusova,[a] Tatyana V. Rybalova,[cd] Evgeny V. Amosov,[c] Mikhail N. Uvarov,[de] Pavel S. Postnikov,*[af] Maxim S. Kazantsev [cd] and Evgeny A. Mostovich**[d]

*a* *Tomsk Polytechnic University, Tomsk 634050, Russia. E-mail: postnikov@tpu.ru*
*b* *Siberian State Medical University, 2, Moskovskiy trakt, Tomsk 634050, Russia.*
*c* *N. N. Vorozhtsov Novosibirsk Institute of Organic Chemistry, Siberian Branch, Russian Academy of Sciences, Novosibirsk 630090, Russia.*
*d* *Novosibirsk State University, Novosibirsk 630090, Russia. E-mail: chemmea@gmail.com*
*e* *V. V. Voevodsky Institute of Chemical Kinetics and Combustion, Siberian Branch, Russian Academy of Sciences, Novosibirsk 630090, Russian Federation.*
*f* *University of Chemistry and Technology, Prague 16628, Czech Republic.*

## Table of contents

# Section S1. Additional experimental spectra

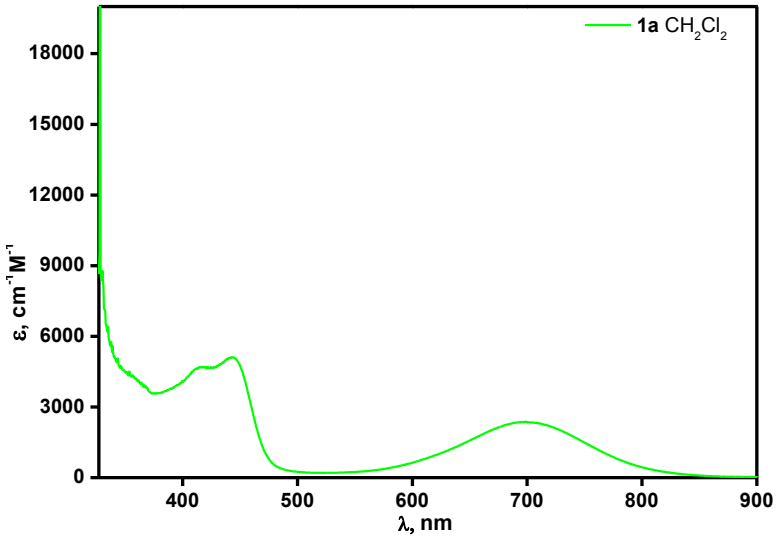


**Fig. S1**. UV-Vis spectrum of **1a** in $CH_2Cl_2$

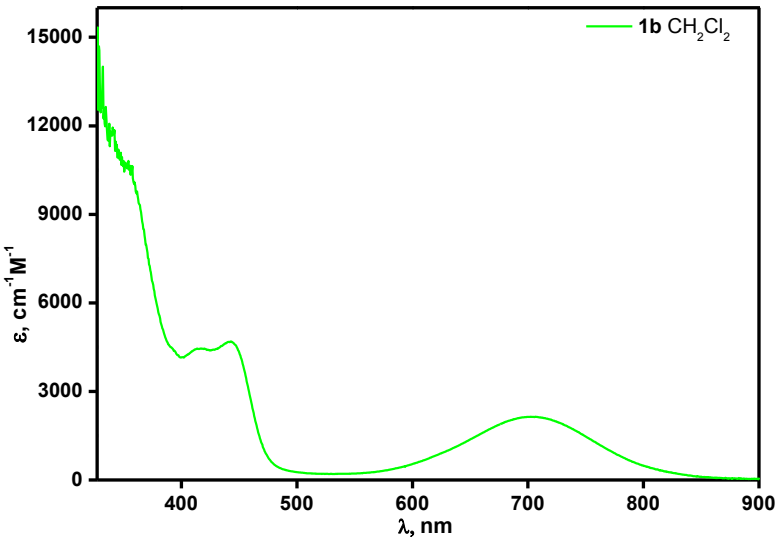


**Fig. S2**. UV-Vis spectrum of **1b** in $CH_2Cl_2$

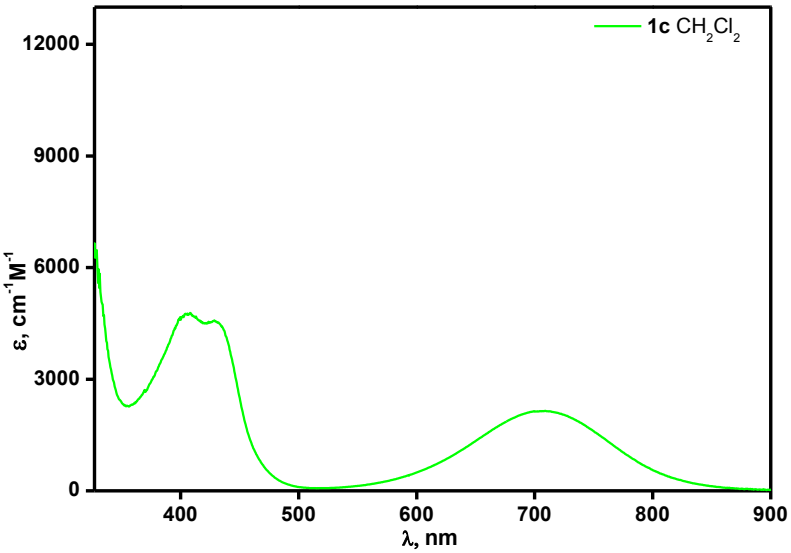


**Fig. S3**. UV-Vis spectrum of **1c** in $CH_2Cl_2$

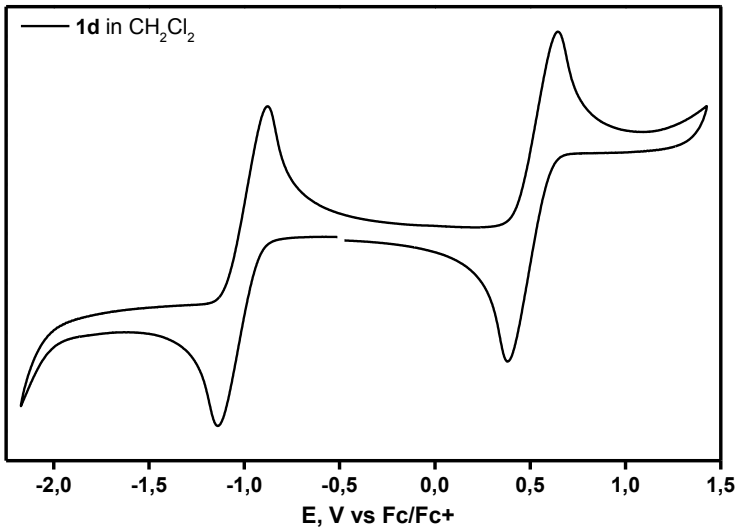


**Fig. S4.** Cyclic voltammogram of **1d** in $CH_2Cl_2$ (100 mV/s with 0.1 M $Bu_4NPF_6$ electrolyte).

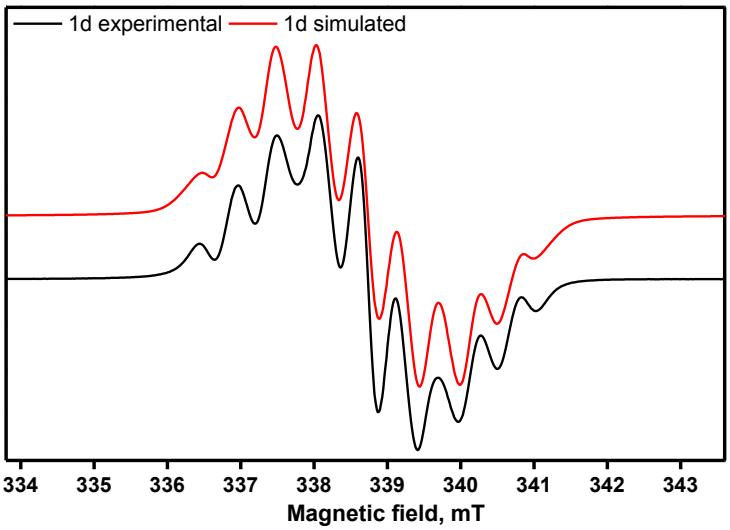


**Fig. S5.** ESR spectra of **1d** (black – experimental, red – simulated) in deoxygenated toluene solution.

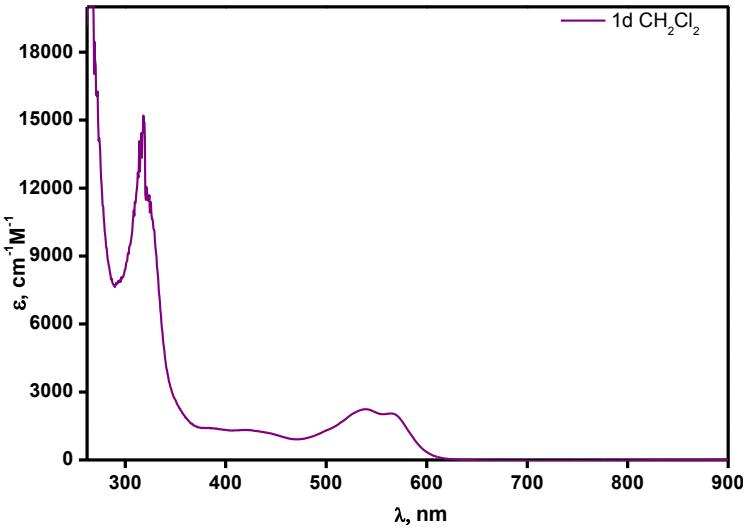


**Fig. S6**. UV-Vis spectrum of **1d** in $CH_2Cl_2$

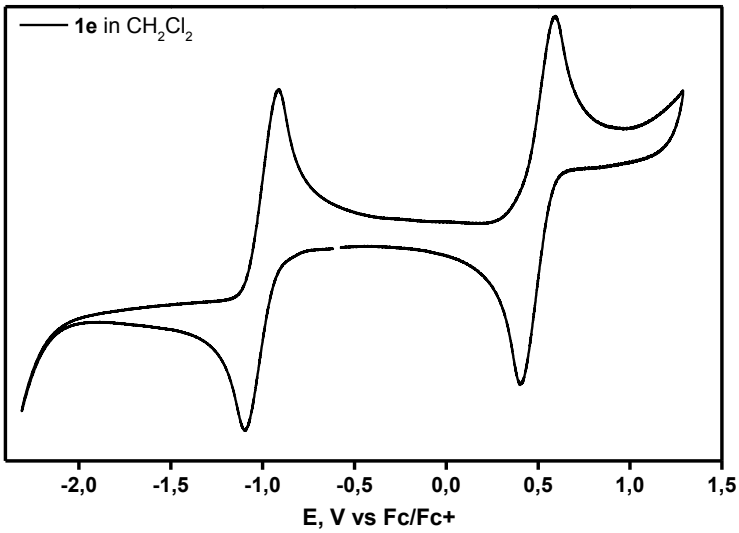


**Fig. S7.** Cyclic voltammogram of **1e** in $CH_2Cl_2$ (100 mV/s with 0.1 M $Bu_4NPF_6$ electrolyte).

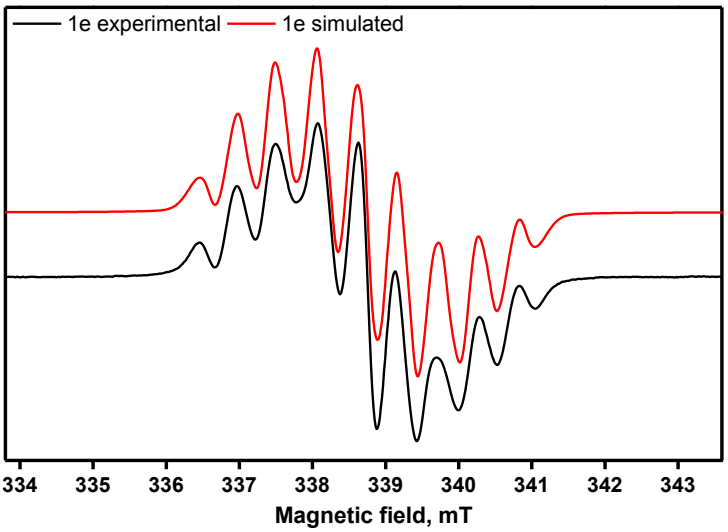


**Fig S8.** ESR spectra of **1e** (black – experimental, red – simulated) in deoxygenated toluene solution.

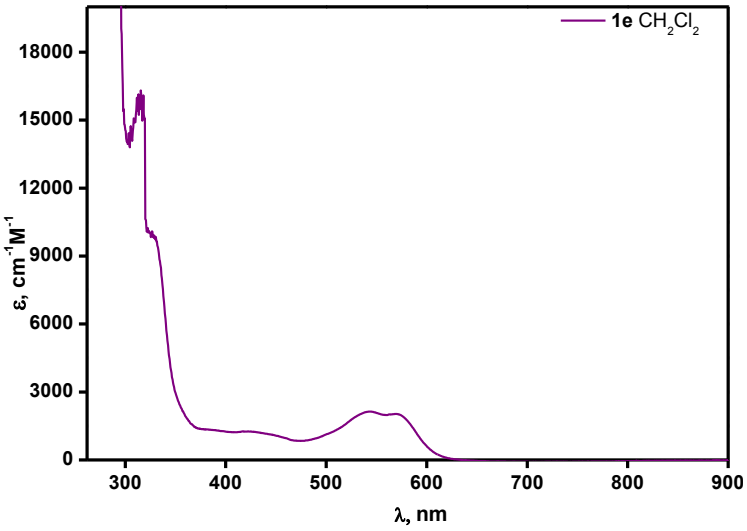


**Fig. S9**. UV-Vis spectrum of **1e** in $CH_2Cl_2$

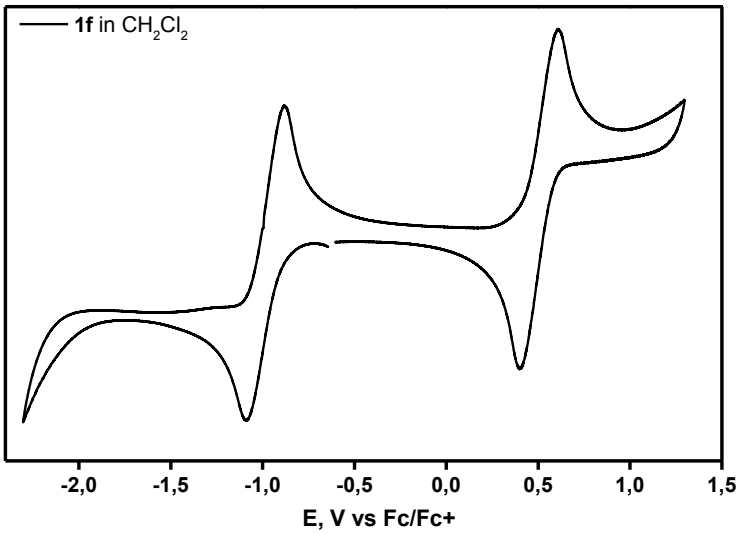


**Fig. S10.** Cyclic voltammogram of **1f** in $CH_2Cl_2$ (100 mV/s with 0.1 M $Bu_4NPF_6$ electrolyte).

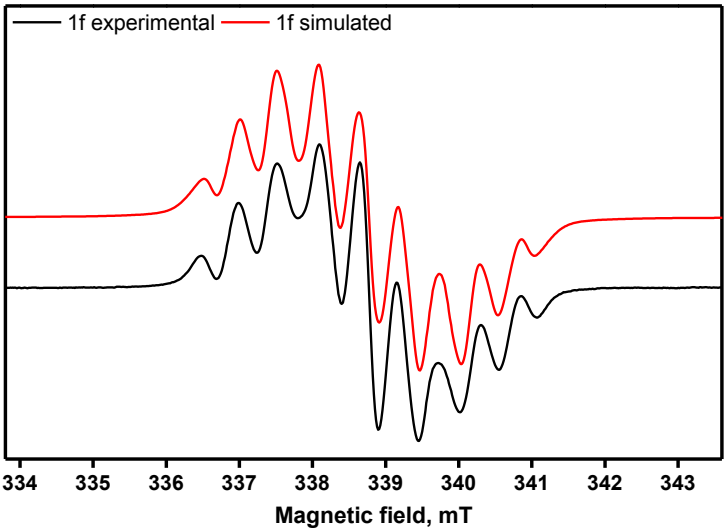


**Fig S11.** ESR spectra of **1f** (black – experimental, red – simulated) in deoxygenated toluene solution.

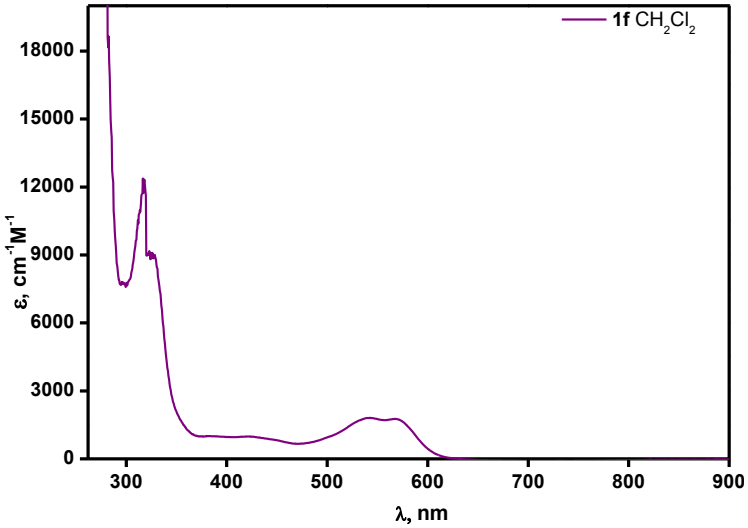


**Fig. S12**. UV-Vis spectrum of **1f** in $CH_2Cl_2$

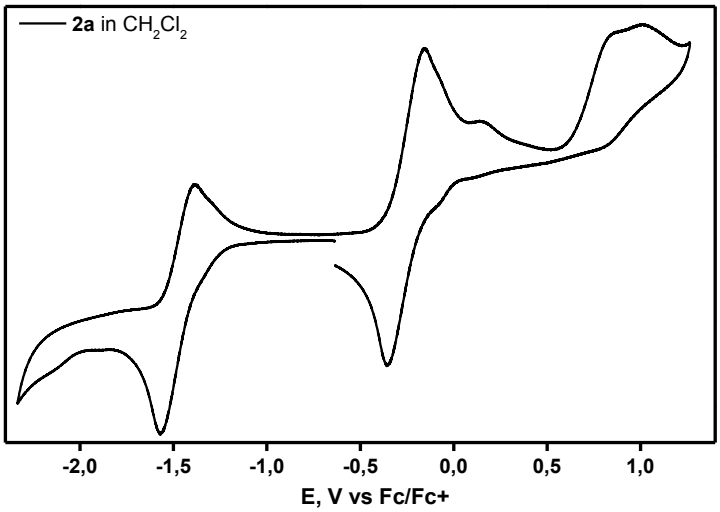


**Fig. S13.** Cyclic voltammogram of **2a** in $CH_2Cl_2$ (100 mV/s with 0.1 M $Bu_4NPF_6$ electrolyte).

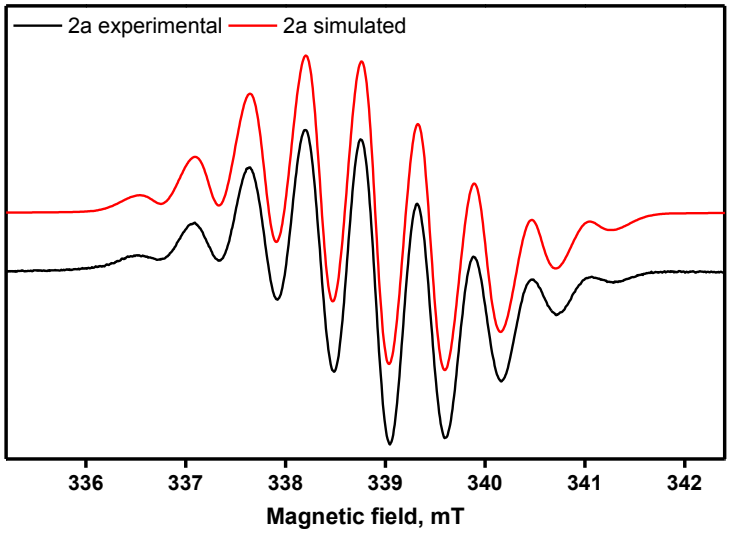


**Fig. S14.** ESR spectra of **2a** (black – experimental, red – simulated) in deoxygenated toluene solution.

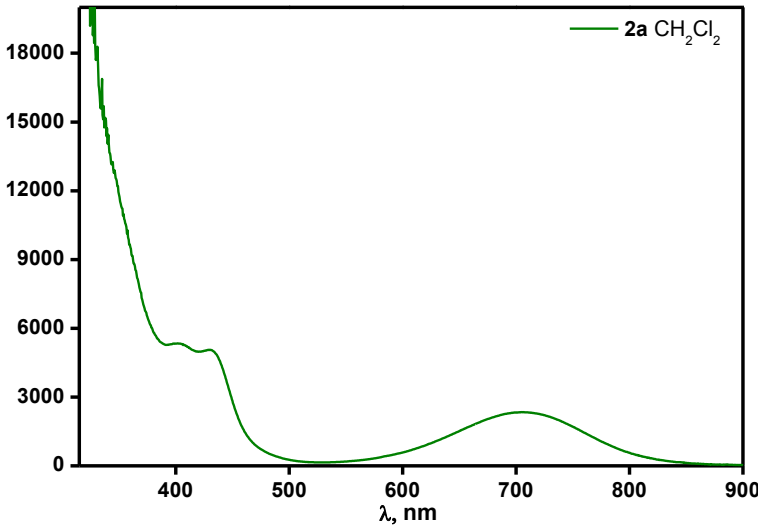


**Fig. S15**. UV-Vis spectrum of **2a** in $CH_2Cl_2$

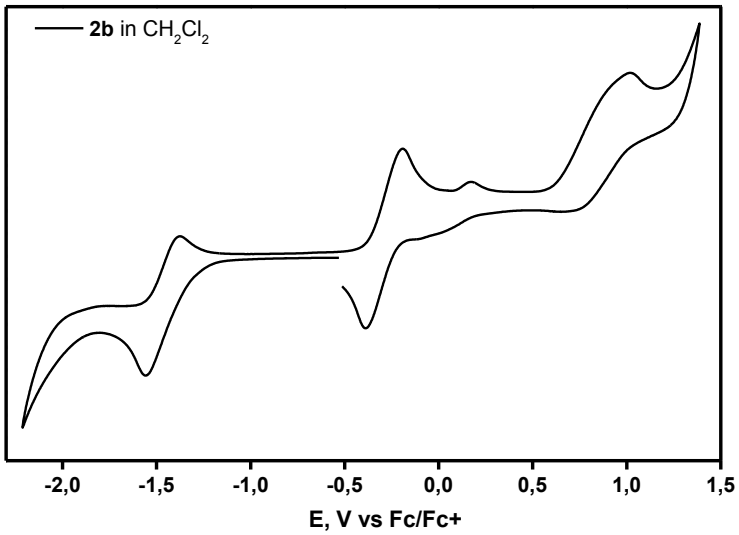


**Fig. S16.** Cyclic voltammogram of **2b** in $CH_2Cl_2$ (100 mV/s with 0.1 M $Bu_4NPF_6$ electrolyte).

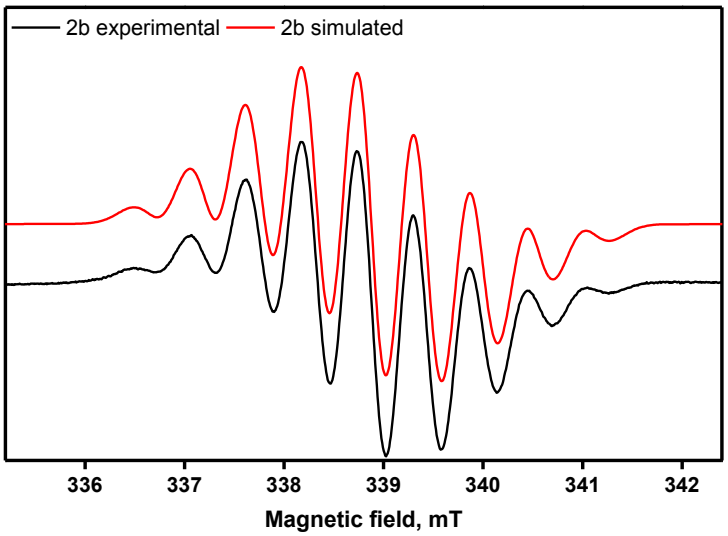


**Fig. S17.** ESR spectra of **2b** (black – experimental, red – simulated) in deoxygenated toluene solution.

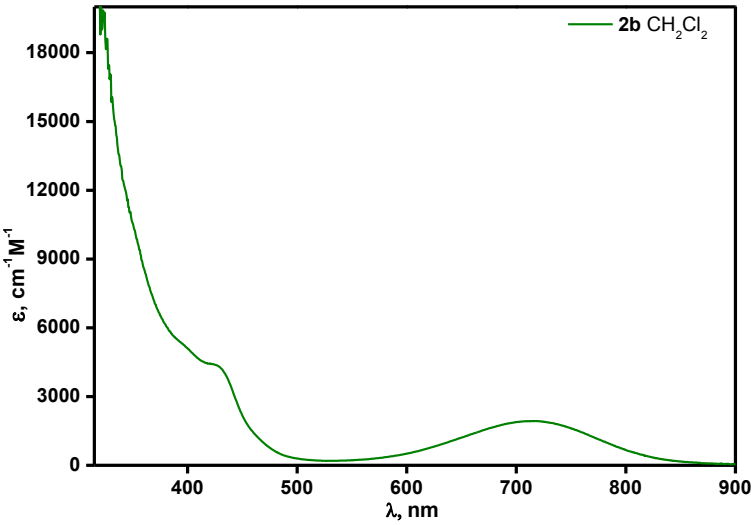


**Fig. S18**. UV-Vis spectrum of **2b** in $CH_2Cl_2$

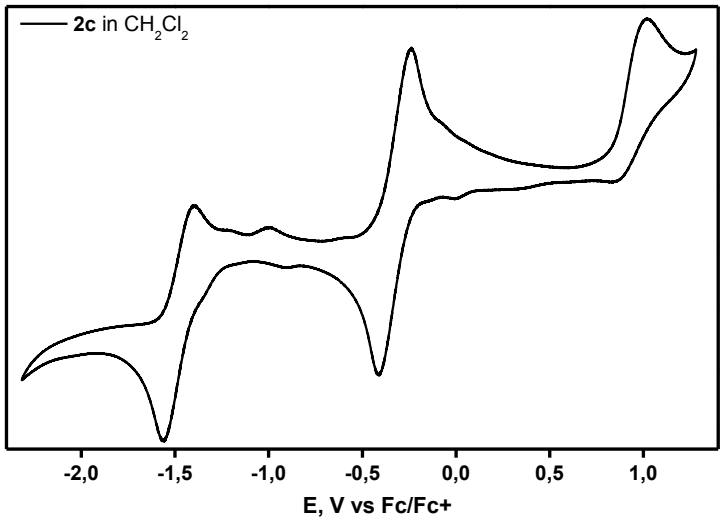


**Fig. S19.** Cyclic voltammogram of **2c** in $CH_2Cl_2$ (100 mV/s with 0.1 M $Bu_4NPF_6$ electrolyte).

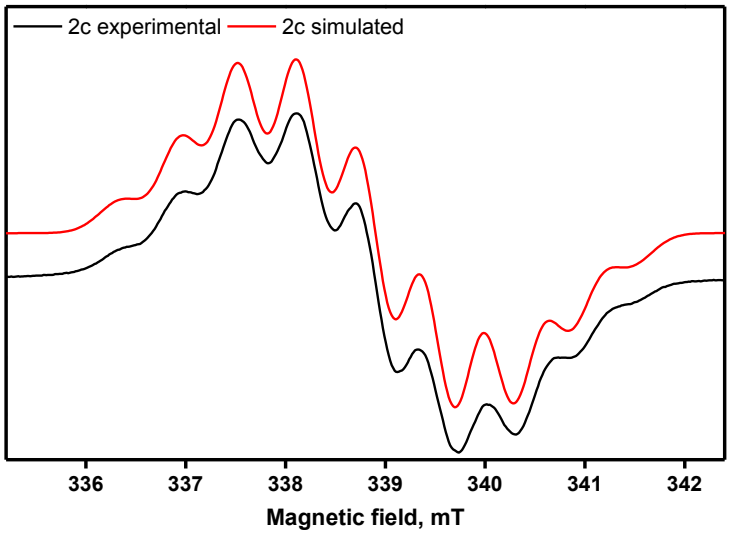


**Fig. S20.** ESR spectra of **2c** (black – experimental, red – simulated) in deoxygenated toluene solution.

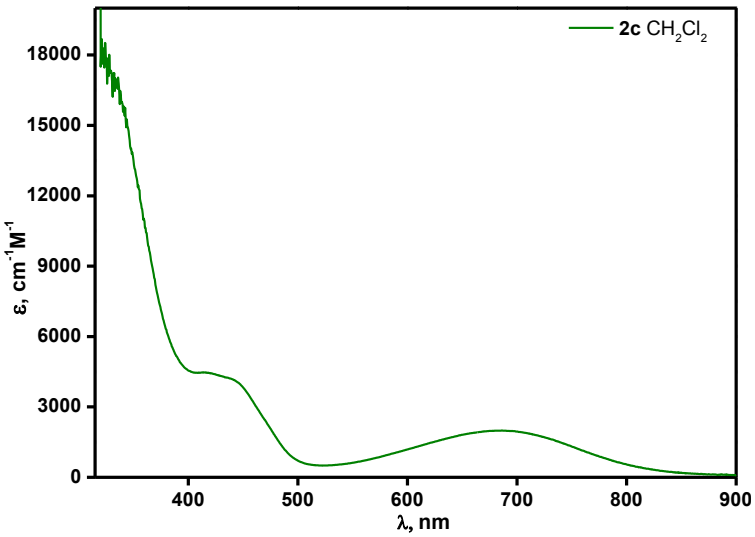


**Fig. S21**. UV-Vis spectrum of **2c** in $CH_2Cl_2$

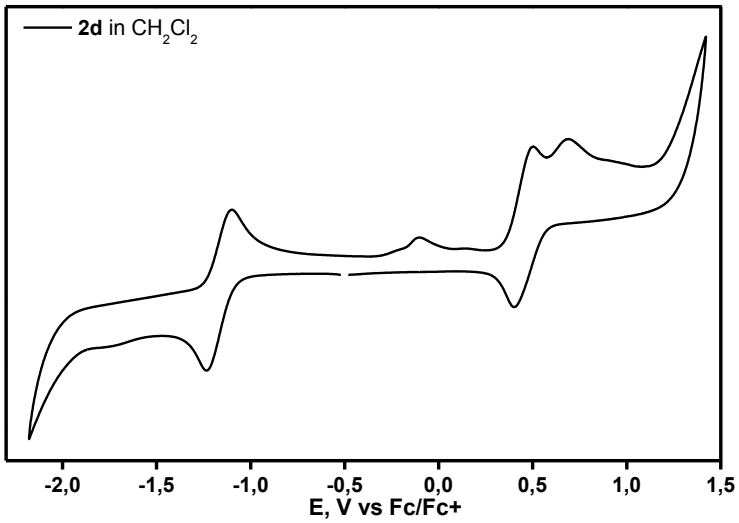


**Fig. S22.** Cyclic voltammogram of **2d** in $CH_2Cl_2$ (100 mV/s with 0.1 M $Bu_4NPF_6$ electrolyte).

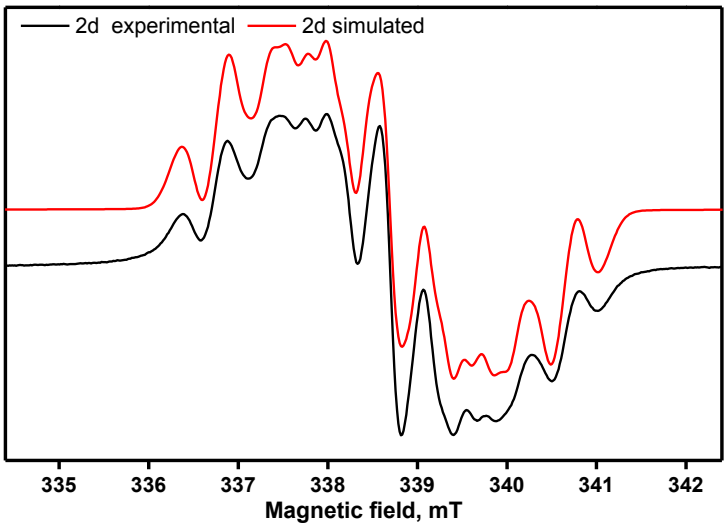


**Fig. S23.** ESR spectra of **2d** (black – experimental, red – simulated) in deoxygenated toluene solution.

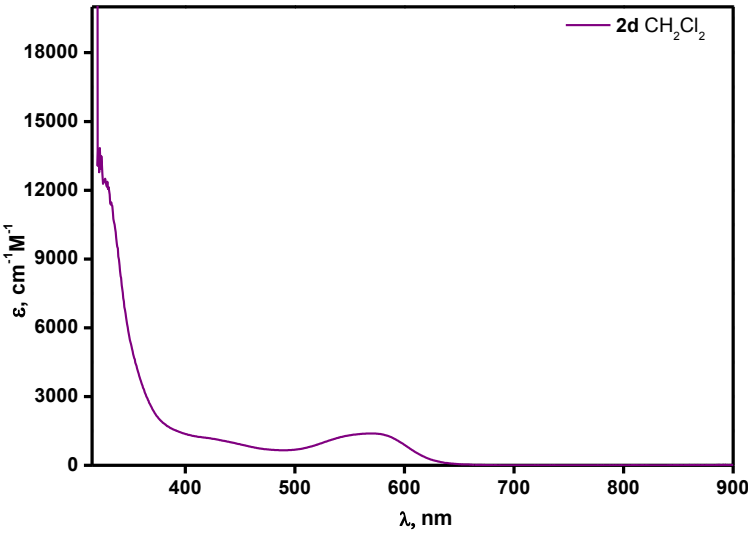


**Fig. S24**. UV-Vis spectrum of **2d** in $CH_2Cl_2$

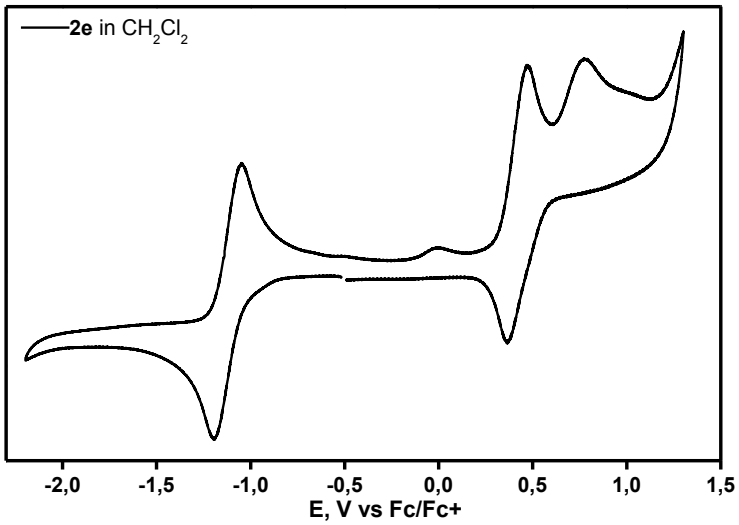


**Fig. S25.** Cyclic voltammogram of **2e** in $CH_2Cl_2$ (100 mV/s with 0.1 M $Bu_4NPF_6$ electrolyte).

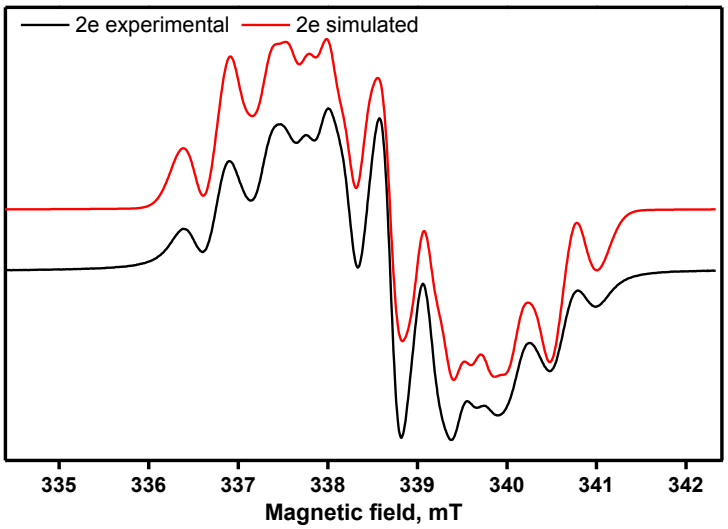


**Fig. S26.** ESR spectra of **2e** (black – experimental, red – simulated) in deoxygenated toluene solution.

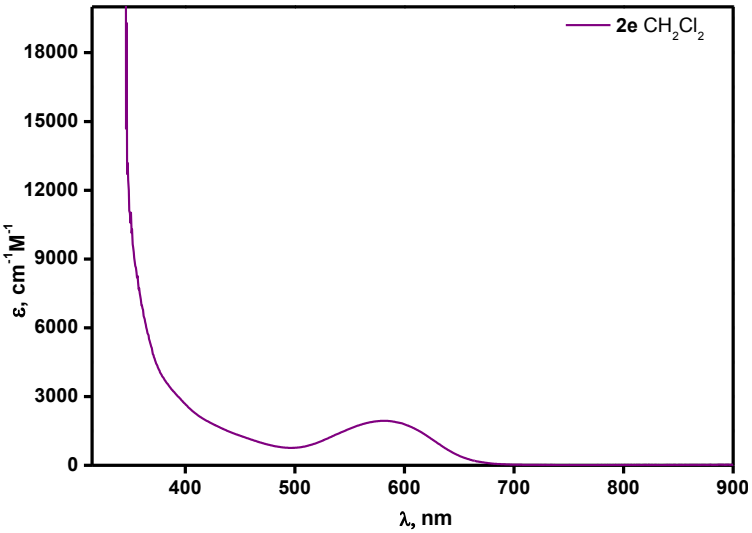


**Fig. S27**. UV-Vis spectrum of **2e** in $CH_2Cl_2$

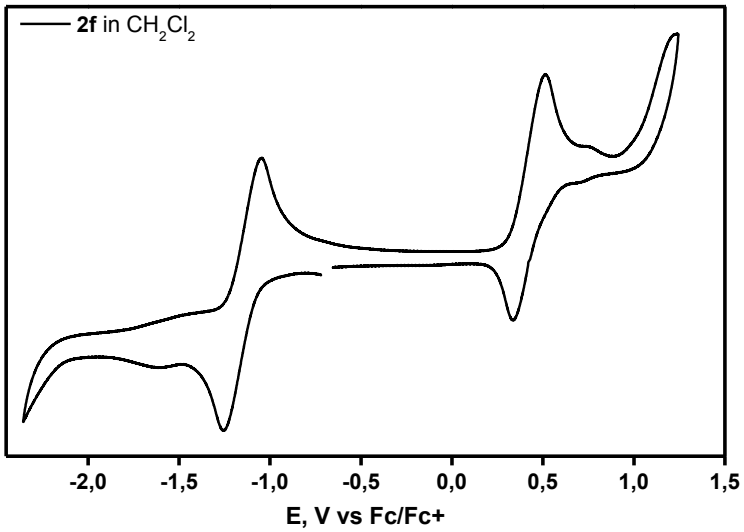


**Fig. S28.** Cyclic voltammogram of **2f** in $CH_2Cl_2$ (100 mV/s with 0.1 M $Bu_4NPF_6$ electrolyte).

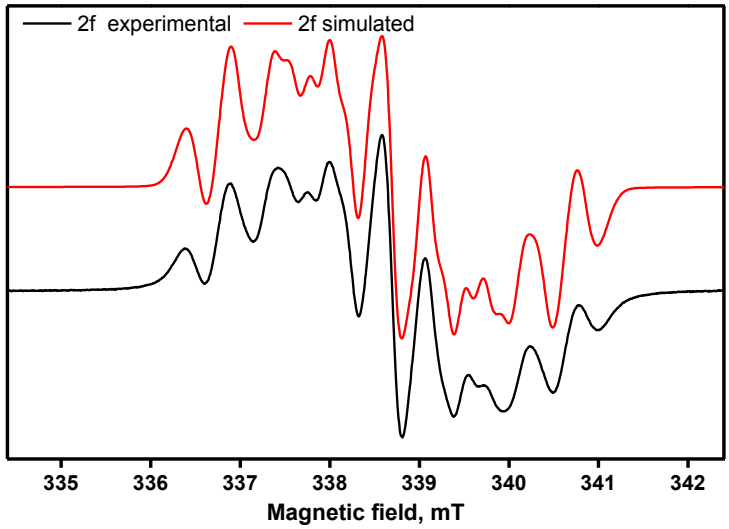


**Fig. S29.** ESR spectra of **2f** (black – experimental, red – simulated) in deoxygenated toluene solution.

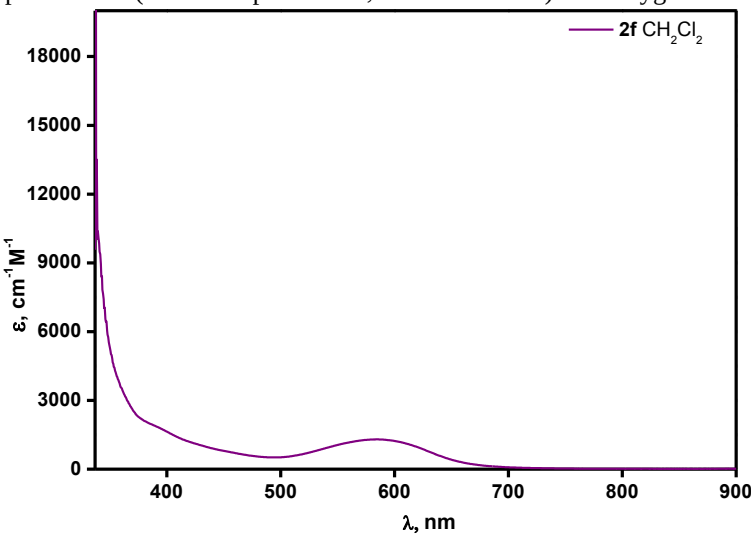


**Fig. S30**. UV-Vis spectrum of **2f** in $CH_2Cl_2$

# Section S2. Full results of oxidative addition reaction

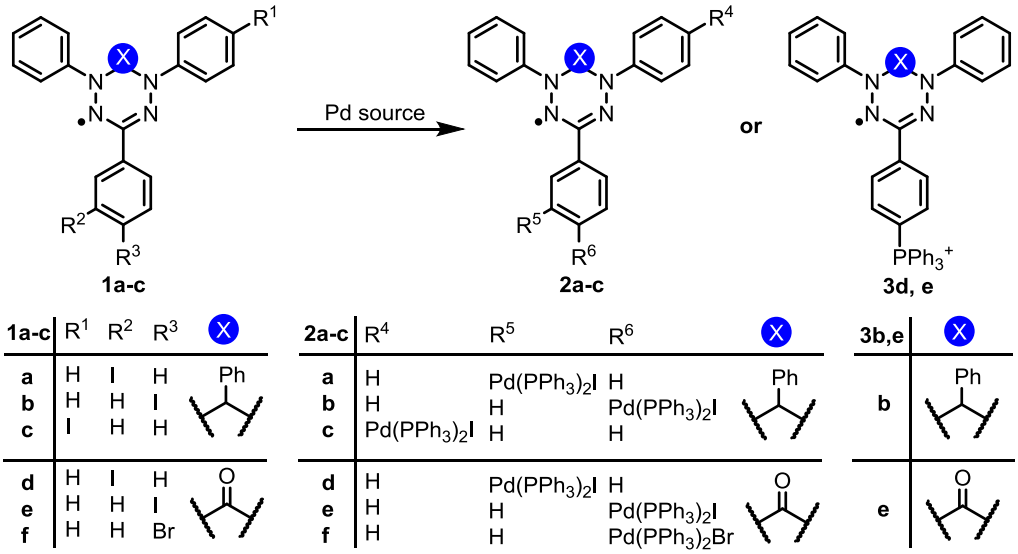


| 1a-c | $R^1$ | $R^2$ | $R^3$ | X |
|---|---|---|---|---|
| a | H | I | H | Ph |
| b | H | H | I | Ph |
| c | I | H | H | Ph |
| d | H | I | H | O |
| e | H | H | I | O |
| f | H | H | Br | O |

| 2a-c | $R^4$ | $R^5$ | $R^6$ | X |
|---|---|---|---|---|
| a | H | $Pd(PPh_3)_2I$ | H | Ph |
| b | H | H | $Pd(PPh_3)_2I$ | Ph |
| c | $Pd(PPh_3)_2I$ | H | H | Ph |
| d | H | $Pd(PPh_3)_2I$ | H | O |
| e | H | H | $Pd(PPh_3)_2I$ | O |
| f | H | H | $Pd(PPh_3)_2Br$ | O |

| 3b,e | X |
|---|---|
| b | Ph |
| e | O |

**Scheme S1.** Synthesis of palladium-verdazyls **2a-2f** from verdazyl radicals **1a-1f**. [a]

| Entry | Reagent/Product | Solvent | [Pd] | Temperature (°C) | Time (h) | Yield (%)[b] | Conversion(%) |
|---|---|---|---|---|---|---|---|
| 1 | **1a/2a** | THF | $Pd(PPh_3)_4$ | 65 | 1 | 91 | >95 |
| 2 | **1b/2b** | THF | $Pd(PPh_3)_4$ | r.t. | 4 | 85 | >95 |
| 3 | **1b/2b** | THF | $Pd(PPh_3)_4$ | 65 | 1 | 90 | >95 |
| 4 | **1b/2b** | toluene | $Pd(PPh_3)_4$ | r.t. | 4 | 83 | 89 |
| 5 | **1b/2b** | toluene | $Pd(PPh_3)_4$ | 65 | 1 | 89 | >95 |
| 6 | **1c/2c** | THF | $Pd(PPh_3)_4$ | 65 | 0.7 | 89 | >95 |
| 7 | **1d/2d** | THF | $Pd(PPh_3)_4$ | 65 | 0.5 | 89 | >95 |
| 8 | **1e/2e** | THF | $Pd(PPh_3)_4$ | r.t. | 2 | 86 | >95 |
| 9 | **1e/2e** | THF | $Pd(PPh_3)_4$ | 65 | 0.5 | 92 | >95 |
| 10 | **1e/2e** | toluene | $Pd(PPh_3)_4$ | r.t. | 2 | 84 | 90 |
| 11 | **1e/2e** | toluene | $Pd(PPh_3)_4$ | 65 | 0.5 | 90 | >95 |
| 12 | **1f/2f** | THF | $Pd(PPh_3)_4$ | 65 | 6 | 5 | 25 |
| 13 | **1f/2f** | THF | $Pd(PPh_3)_4$ | 65 | 12 | 25 | 45 |
| 14 | **1f/2f** | THF | $Pd(PPh_3)_4$ | 65 | 24(48) | 39(39) | 59(61) |
| 15 | **1f/2f** | toluene | $Pd(PPh_3)_4$ | 65 | 24(48) | 37(37) | 54(55) |
| 16[c] | **1b/2b** | THF | $Pd(PPh_3)_4$ | 65 | 1 | traces | >95 |
| 17[d] | **1b/2b** | THF | $Pd(PPh_3)_2Cl_2$ | 65 | 2 | 91% of **3b** | >95 |
| 18[d] | **1e/2e** | THF | $Pd(PPh_3)_2Cl_2$ | 65 | 2 | 88% of **3e** | >95 |
| 19 | **1b/2b** | $CH_3CN$ | $Pd(CH_3CN)_2Cl_2$ | r.t. | 4 | decomp. | >95 |
| 20[e] | **1b** with **Ph-C≡CH/2b** | THF | $Pd(PPh_3)_2Cl_2$ | 65 | 2 | 48% of **2b;** 40% of **3b** | >95 |
| 21[e] | **1e** with **Ph-C≡CH/2e** | THF | $Pd(PPh_3)_2Cl_2$ | 65 | 2 | 53% of **2e;** 34% of **3e** | >95 |

[a] Optimized conditions: iodine-containing verdazyl (0.1 mmol) and $Pd(PPh_3)_4$ (0.1 mmol) were mixed in deoxygenated THF (5 ml); reaction progress was monitored by TLC; [b] isolated yields; [c] $NEt_3$ was added; [d] verdazyl-$PPh_3^+$ **3** was observed as product according to HRMS analysis; [e] 1 eq. of phenylacetylene was added

## Section S3. X-ray data

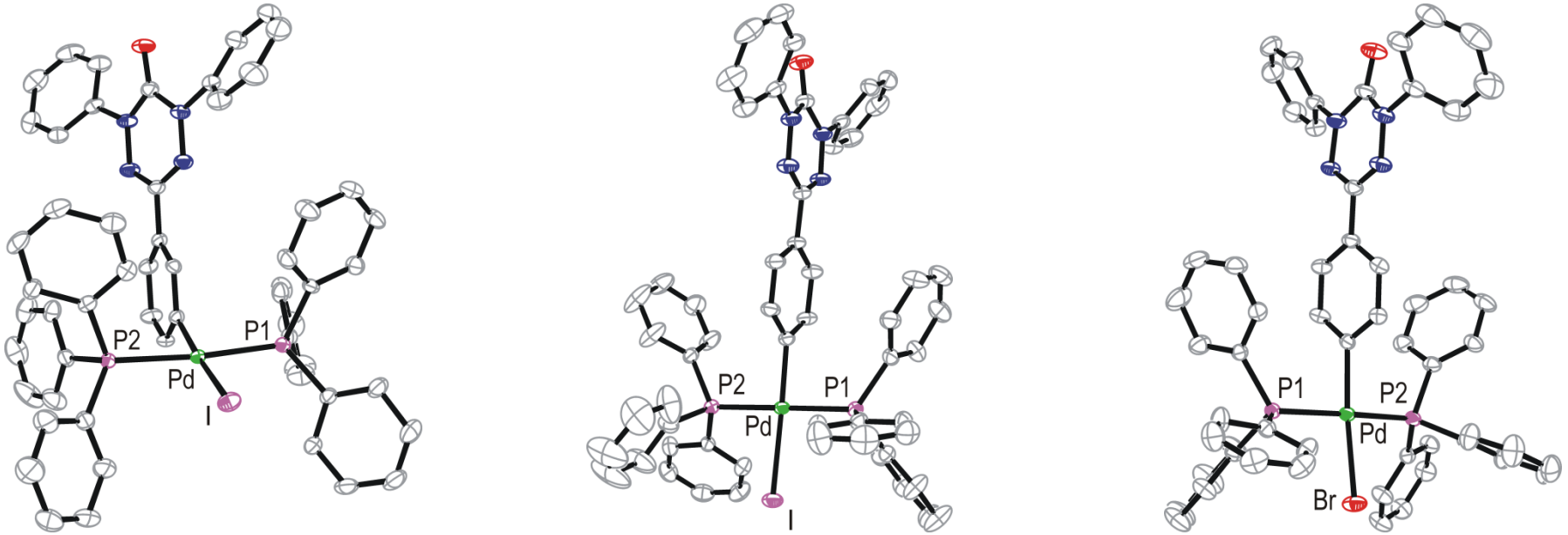


**Fig. S31** Molecular structure of **2d** (left)**, 2e** (center)**, 2f** (right)**.** Thermal ellipsoids drawn at 30% probability. The minor part of disordered phenyl cycles in **2e** is omitted for clarity

Structural comparison of **2d,2e,2f** with previously reported diamagnetic palladium intermediates iodo-phenyl-bis(triphenylphosphine)-palladium(II)[1] and bromo-(4-ethylphenyl)-bis(triphenylphosphine)-palladium(II)[2] shows differences in bond lengths no more than 0.02 Å and very similar bond angles (Table S1). Thus, conjugation with paramagnetic center does not make any sufficient impact on the structure of oxidative addition intermediates.

**Table S1**. Selected bond lengths and angles of complexes **2d, 2e, 2f** and known palladium intermediates.

| | **2d** | **2e** | Iodo-phenyl-bis(triphenylphosphine)-palladium(II) [1] | **2f** | bromo-(4-ethylphenyl)-bis(triphenylphosphine)-palladium(II) [2] |
|---|---|---|---|---|---|
| *Bond lengths, Å* | | | | | |
| Pd – Hal | 2.6905(7) | 2.6976(5) | 2.7010(9) | 2.5132(5) | 2.5215(4) |
| Pd – P1 | 2.339(2) | 2.321(1) | 2.342(1) | 2.3387(8) | 2.3225(7) |
| Pd – P2 | 2.336(2) | 2.3225(9) | 3.337(1) | 2.3445(9) | 2.3346(7) |
| Pd – C | 2.012(5) | 2.016(3) | 2.029(4) | 2.023(3) | 2.028(3) |
| *Angles, degrees* | | | | | |
| C – Pd – Hal | 172.8(2) | 172.51(9) | 171.4(1) | 169.9(1) | 178.80 |
| P1 – Pd – P2 | 173.62(5) | 178.17(3) | 173.81(4) | 173.00(3) | 178.72 |

**Table S2.** Crystal data and structure refinement details for compounds **2d, 2e, 2f.**

| | Compound | | |
|---|---|---|---|
| | **2d** | **2e** | **2f** |
| Empirical formula | $C_{56}H_{44}IN_4OP_2Pd$·solvent | $C_{56}H_{44}IN_4OP_2Pd$·½[$CH_2Cl_2$] | $C_{56}H_{44}BrN_4OP_2Pd$·0.84[$CH_2Cl_2$] |
| Formula weight | 1084.19 | 1126.65 | 1108.79 |
| Temperature K | 296(2) | 296(2) | 296(2) |
| Crystal system | Triclinic | Triclinic | Triclinic |
| Space group | P-1 | P-1 | P-1 |
| Unit cell dimensions *a* Å | 9.2359(6) | 12.4819(5) | 10.7741(3) |
| *b* Å | 11.991(1) | 15.2493(6) | 12.8315(4) |
| *c* Å | 23.858(2) | 15.4903(6) | 19.8161(6) |
| *α* | 85.044(4) | 65.585(2) | 92.147(2) |
| *β* ° | 81.344(3) | 82.390(2) | 98.758(2) |
| *γ* | 75.570(4) | 73.138(2) | 109.794(2) |
| Volume Å$^3$ | 2526.4(3) | 2569.07(18) | 2535.9(1) |
| *Z* | 2 | 2 | 2 |
| Density (calcd.) g.cm$^{-3}$ | 1.425 | 1.456 | 1.452 |
| Absorption coefficient mm$^{-1}$ | 1.084 | 1.119 | 1.350 |
| F(000) | 1090 | 1132 | 1124.8 |
| Crystal size mm$^3$ | 0.45 × 0.14 × 0.02 | 0.34 × 0.17 × 0.04 | 0.33 × 0.32 × 0.20 |
| Θ range for data collection ° | 2.30 − 25.98 | 2.22 − 28.81 | 2.30 − 26.74 |
| Index ranges | $-10 \le h \le 10$, $-14 \le k \le 14$, $-28 \le l \le 28$ | $-16 \le h \le 16$, $-20 \le k \le 20$, $-20 \le l \le 20$ | $-13 \le h \le 13$, $-16 \le k \le 16$, $-25 \le l \le 25$ |
| Reflections collected | 38930 | 80953 | 45234 |
| Independent reflections [Rint] | 8857 [0.0416] | 13396 [0.0468] | 10747 [0.0309] |
| Reflections observed (I > 2σ(I)) | 7200 | 8983 | 8481 |
| Completeness to θ % | 99.4 | 99.9 | 99.6 |
| Data / restraints / parameters | 8857 / 0 / 586 | 13396 / 20 / 646 | 10747 /2 / 614 |
| Goodness-of-fit on F$^2$ | 1.090 | 1.029 | 1.008 |
| Final R indices I > 2σ(I), *R*1 / *wR*2 | 0.0488 / 0.1271 | 0.0406 / 0.0879 | 0.0403 / 0.1073 |
| Final R indices (all data), *R*1 / | 0.0634 / 0.1324 | 0.0790 / 0.1050 | 0.0588 / 0.1243 |
| Largest diff. peak / hole e.Å$^{-3}$ | 0.788 / -1.061 | 0.936 / -0.801 | 1.203 / -0.688 |

## Section S4. ESR data

Spectra of meta- and para-substituted radicals were similar for substances: **1a**, **1b** and **1c**; **1d, 1e** and **1f**; **2a** and **2b**; **2d**, **2e** and **2f**. The values of g-factors and constants of hyperfine interaction between the electron spin and nitrogen nuclear which has been obtained after the numerical simulation of the ESR spectra are shown in Table S3.

**Table S3**. ESR parameters of **1a-1f** and **2a-2f**

| | **1a** | **2a** | **1b** | **2b** | **1c** | **2c** | **1d** | **2d** | **1e** | **2e** | **1f** | **2f** |
|---|---|---|---|---|---|---|---|---|---|---|---|---|
| g-factor | 2.0034 | 2.0033 | 2.0033 | 2.0035 | 2.0038 | 2.0038 | 2.0039 | 2.0038 | 2.0039 | 2.0038 | 2.0039 | 2.0038 |
| $a_{N1}$, G | 5.41 | 5.25 | 5.48 | 5.25 | 5.36 | 7.06 | 4.59 | 4.42 | 4.59 | 4.36 | 4.60 | 4.35 |
| $a_{N2}$, G | 5.41 | 5.72 | 5.48 | 5.75 | 5.35 | 5.40 | 6.10 | 6.52 | 6.15 | 6.40 | 6.13 | 6.40 |
| $a_{N4}$, G | 5.41 | 5.72 | 5.48 | 5.75 | 5.35 | 5.40 | 6.10 | 6.52 | 6.15 | 6.40 | 6.13 | 6.40 |
| $a_{N5}$, G | 5.41 | 5.25 | 5.48 | 5.25 | 5.36 | 5.40 | 4.59 | 4.42 | 4.59 | 4.36 | 4.60 | 4.35 |
| ILB, G [a] | 2.23 | 2.30 | 2.09 | 2.11 | 2.24 | 2.31 | 2.20 | 1.73 | 1.89 | 1.73 | 1.93 | 1.67 |

a Value of individual line broadening which was used for simulation of ESR spectra in Winsim2002 software

## Section S5. Electrochemical properties

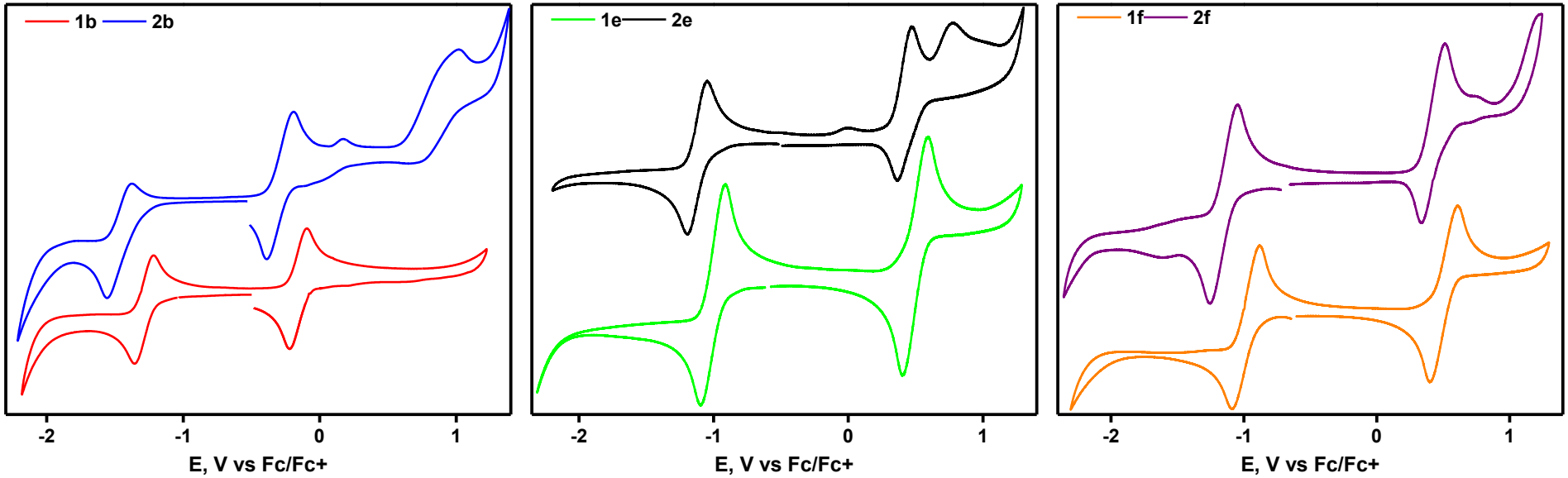


**Fig. S32** Cyclic voltammograms of **1b** (red) *vs.* **2b** (blue), **1e** (green) *vs.* **2e** (black) and **1f** (orange) *vs.* **2f** (violet) in $CH_2Cl_2$ (100 mV/s with 0.1 M $Bu_4NPF_6$ electrolyte).

**Table S4.** Electrochemical properties of starting radicals **1a-1f** and Pd-derivatives **2a-2f** [a]

| Compound | $E_{Red}^{1/2}$, V | $E_{Ox}^{1/2}$, V | Compound | $E_{Red}^{1/2}$, V | $E_{Ox1}^{1/2}$, V | $E_{Ox2}^{1/2}$, V |
|---|---|---|---|---|---|---|
| **1a** | -1.31 | -0.16 | **2a** | -1.48 | -0.26 | 1.03[b] |
| **1b** | -1.29 | -0.16 | **2b** | -1.47 | -0.29 | 1.02[b] |
| **1c** | -1.23 | -0.16 | **2c** | -1.47 | -0.33 | 1.03[b] |
| **1d** | -1.01 | 0.51 | **2d** | -1.17 | 0.45 | 0.69[b] |
| **1e** | -1.01 | 0.50 | **2e** | -1.12 | 0.42 | 0.78[b] |
| **1f** | -0.98 | 0.50 | **2f** | -1.15 | 0.42 | - |

[a] Potentials are reported in V vs $Fc/Fc^+$. [b] Irreversible process, cathodic peak potentials are given.

## Section S6. NMR spectra

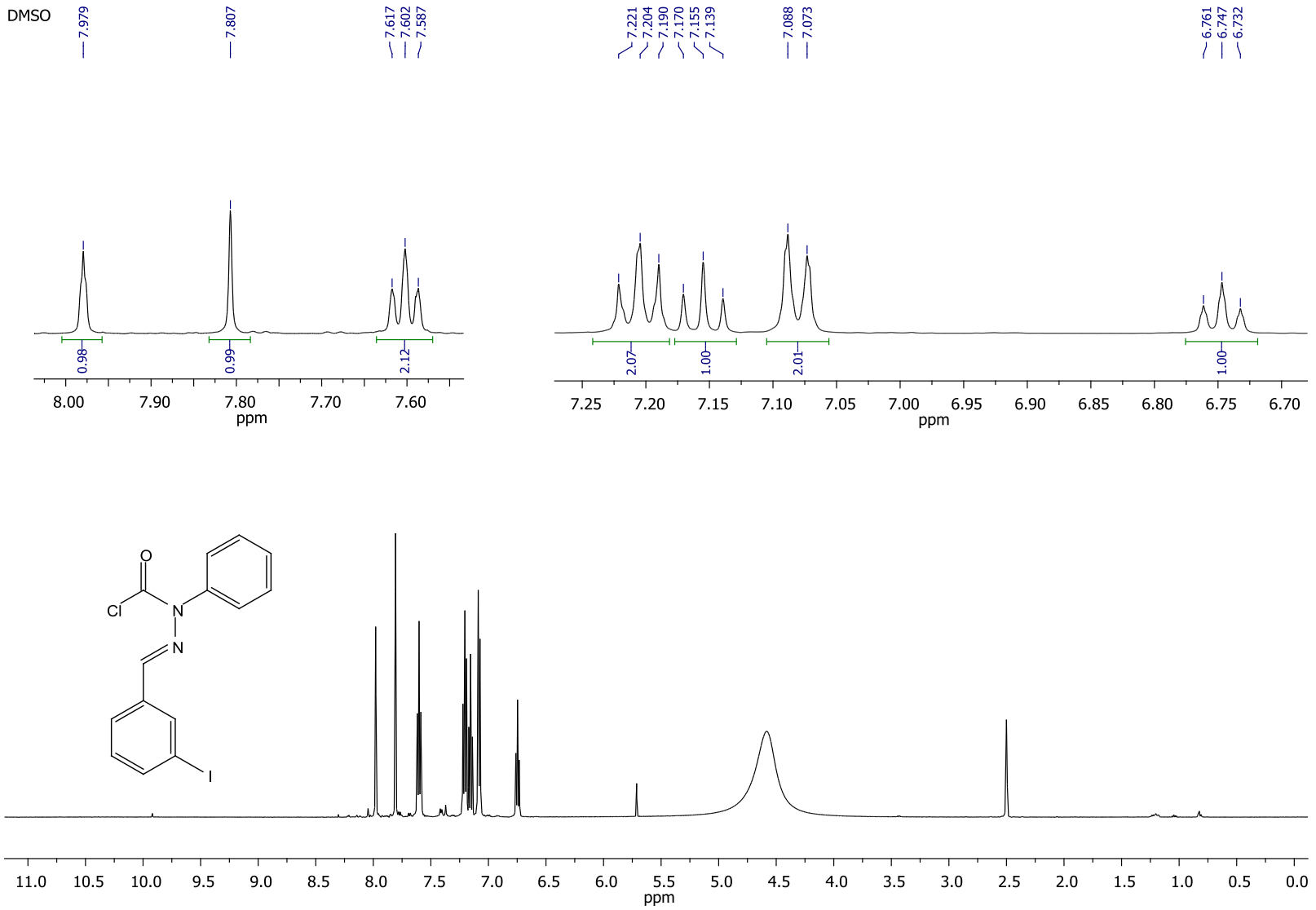


**Fig. S33** $^{1}$H NMR spectrum (DMSO-d6) of 2-(3-iodophenyl)-α-chloroformyl-4-phenylhydrazone **6d.**

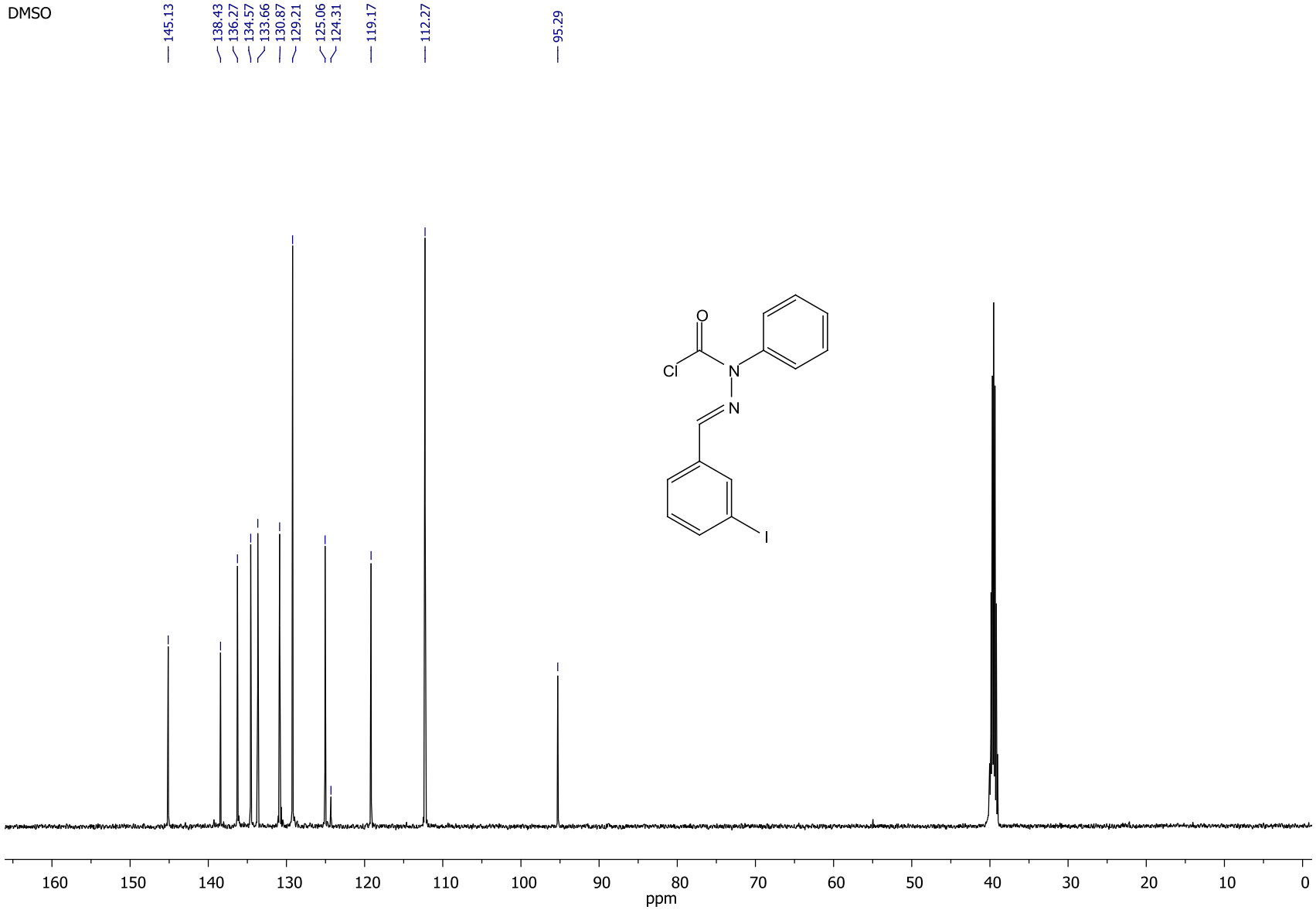


**Fig. S34** $^{13}$C NMR spectrum (DMSO-d6) of 2-(3-iodophenyl)-α-chloroformyl-4-phenylhydrazone **6d.**

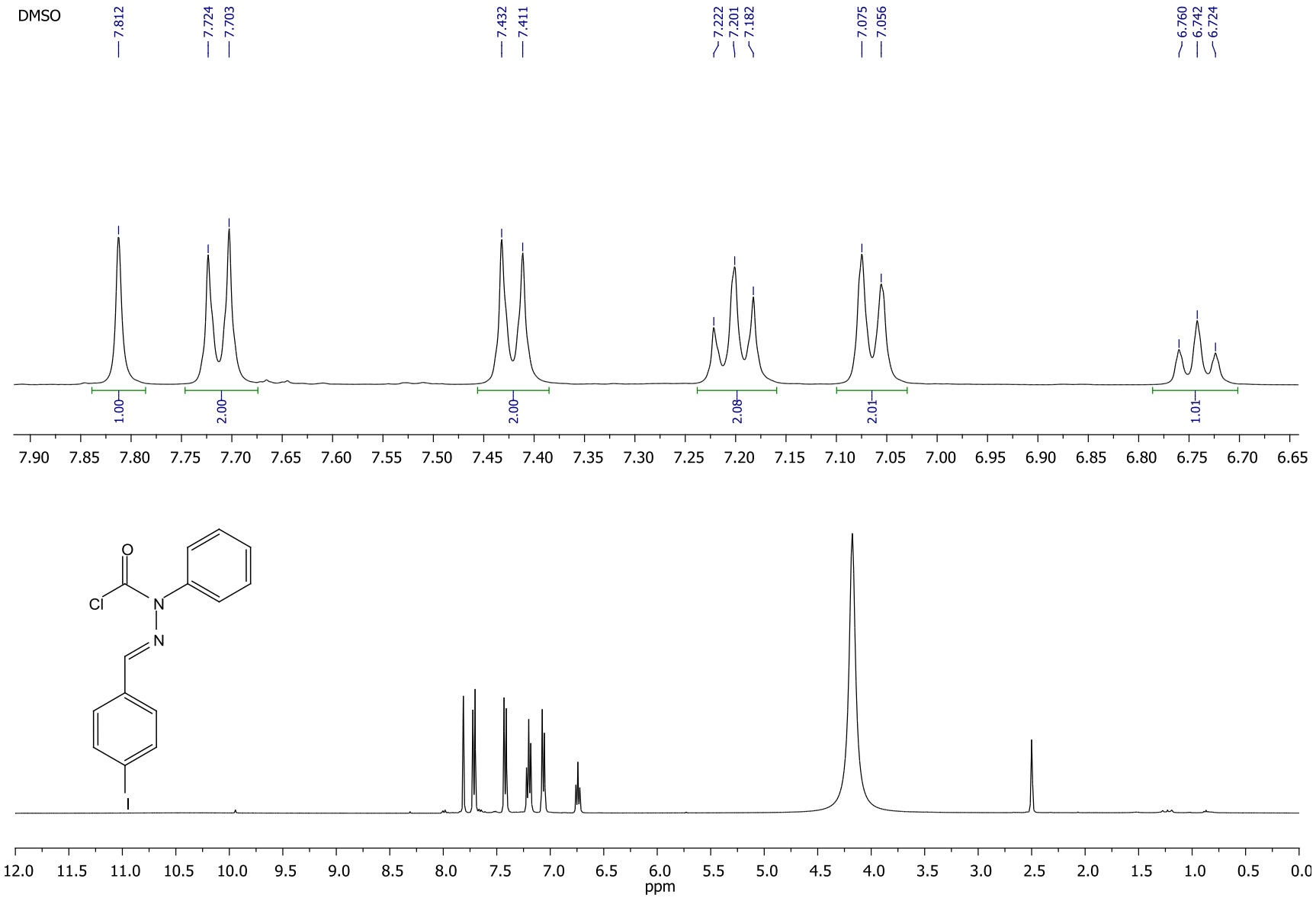


**Fig. S35** $^{1}$H NMR spectrum (DMSO-d6) of 2-(4-iodophenyl)-α-chloroformyl-4-phenylhydrazone **6e.**

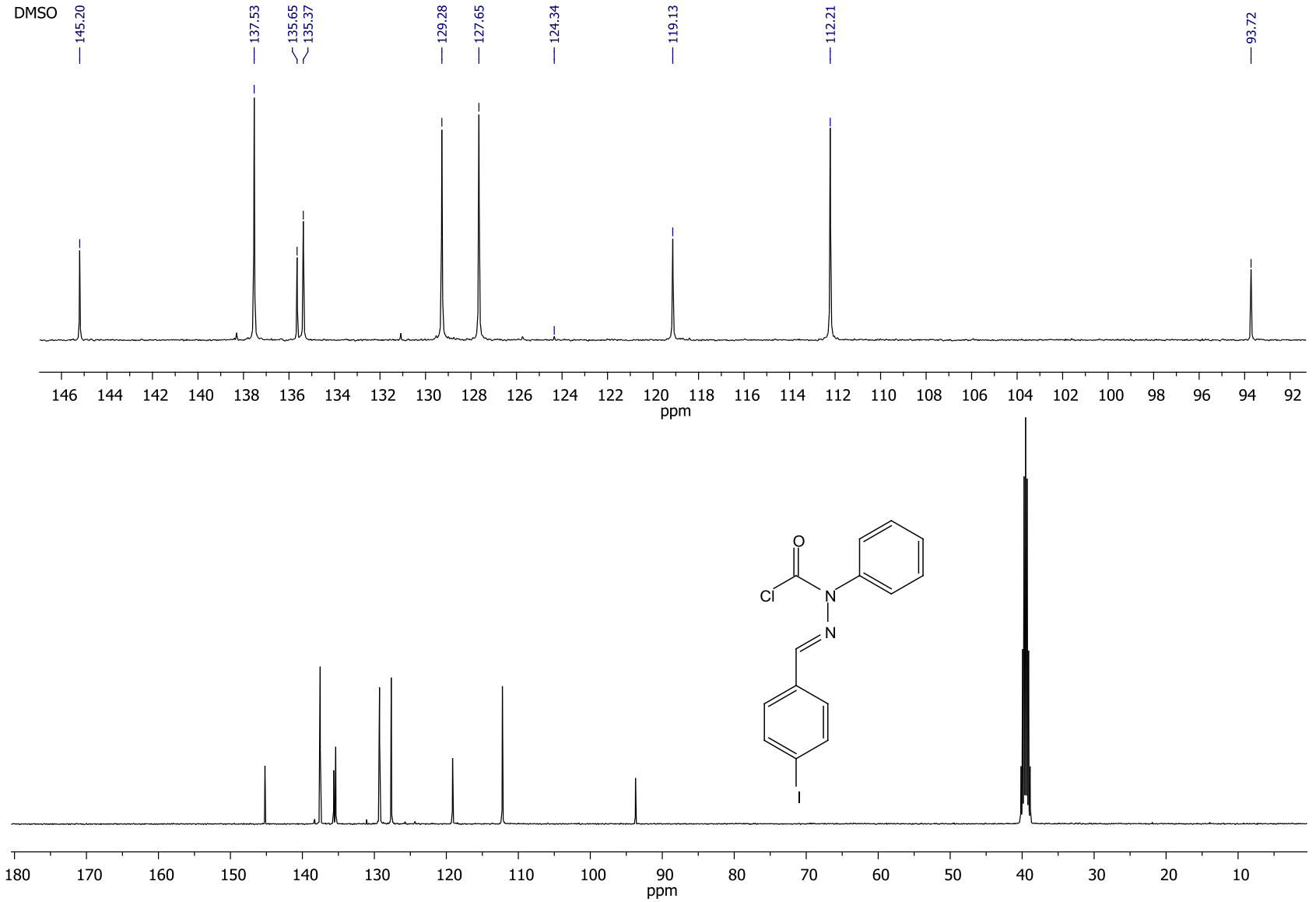


**Fig. S36** $^{13}$C NMR spectrum (DMSO-d6) of 2-(4-iodophenyl)-α-chloroformyl-4-phenylhydrazone **6e.**

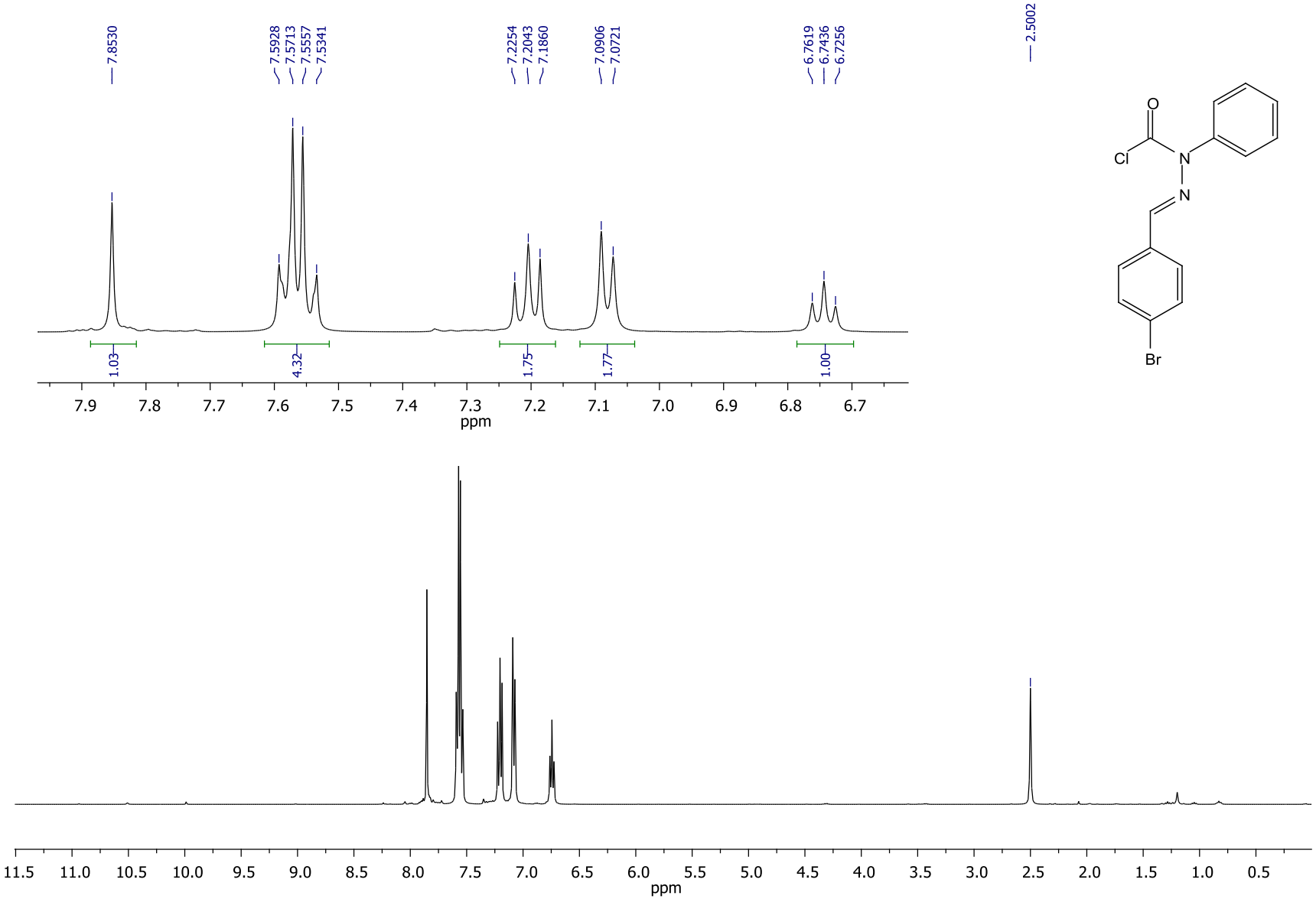


**Fig. S37** $^{1}$H NMR spectrum (DMSO-d6) of 2-(4-bromophenyl)-α-chloroformyl-4-phenylhydrazone **6f.**

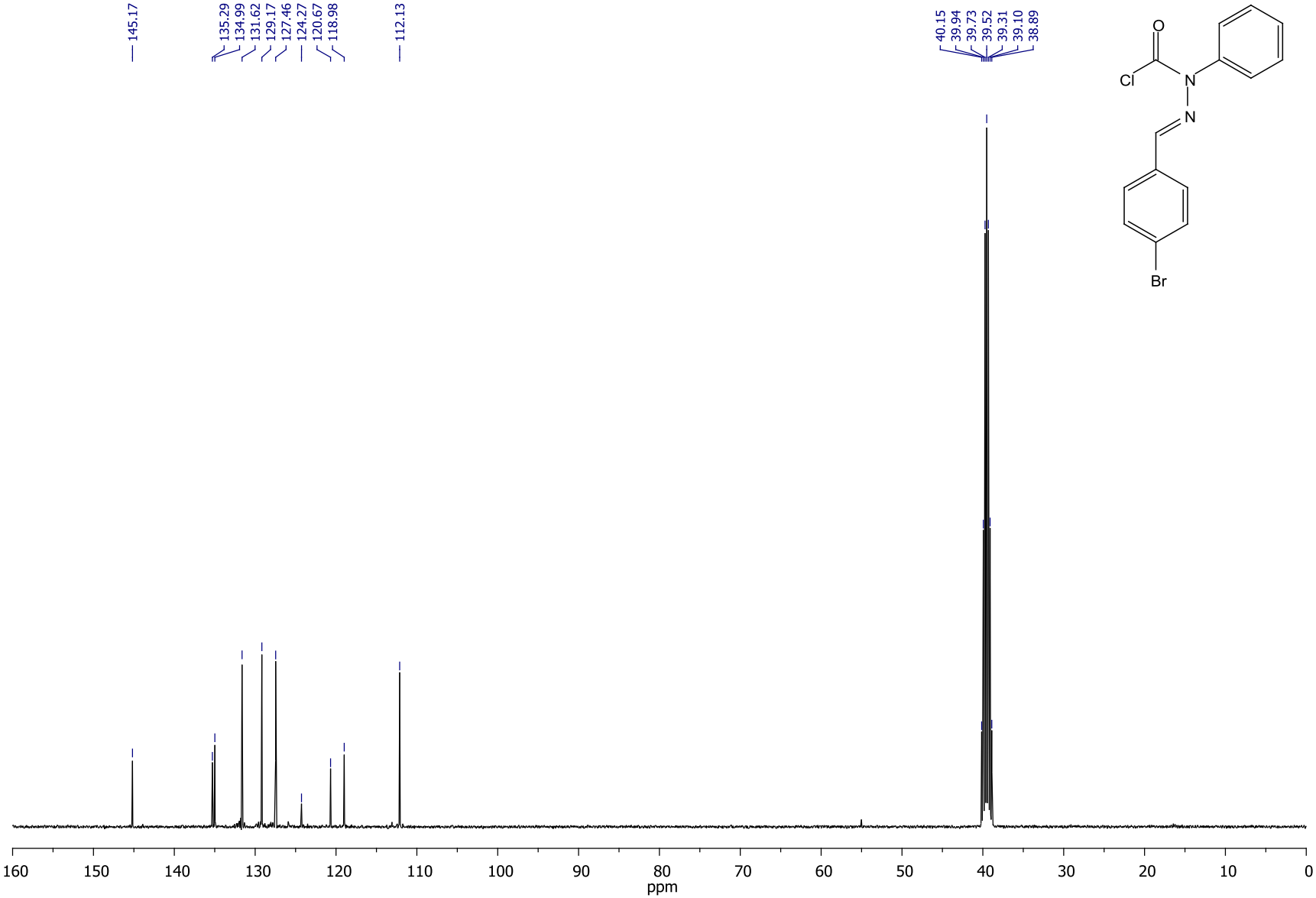


**Fig. S38** $^{13}$C NMR spectrum (DMSO-d6) of 2-(4-bromophenyl)-α-chloroformyl-4-phenylhydrazone **6f.**

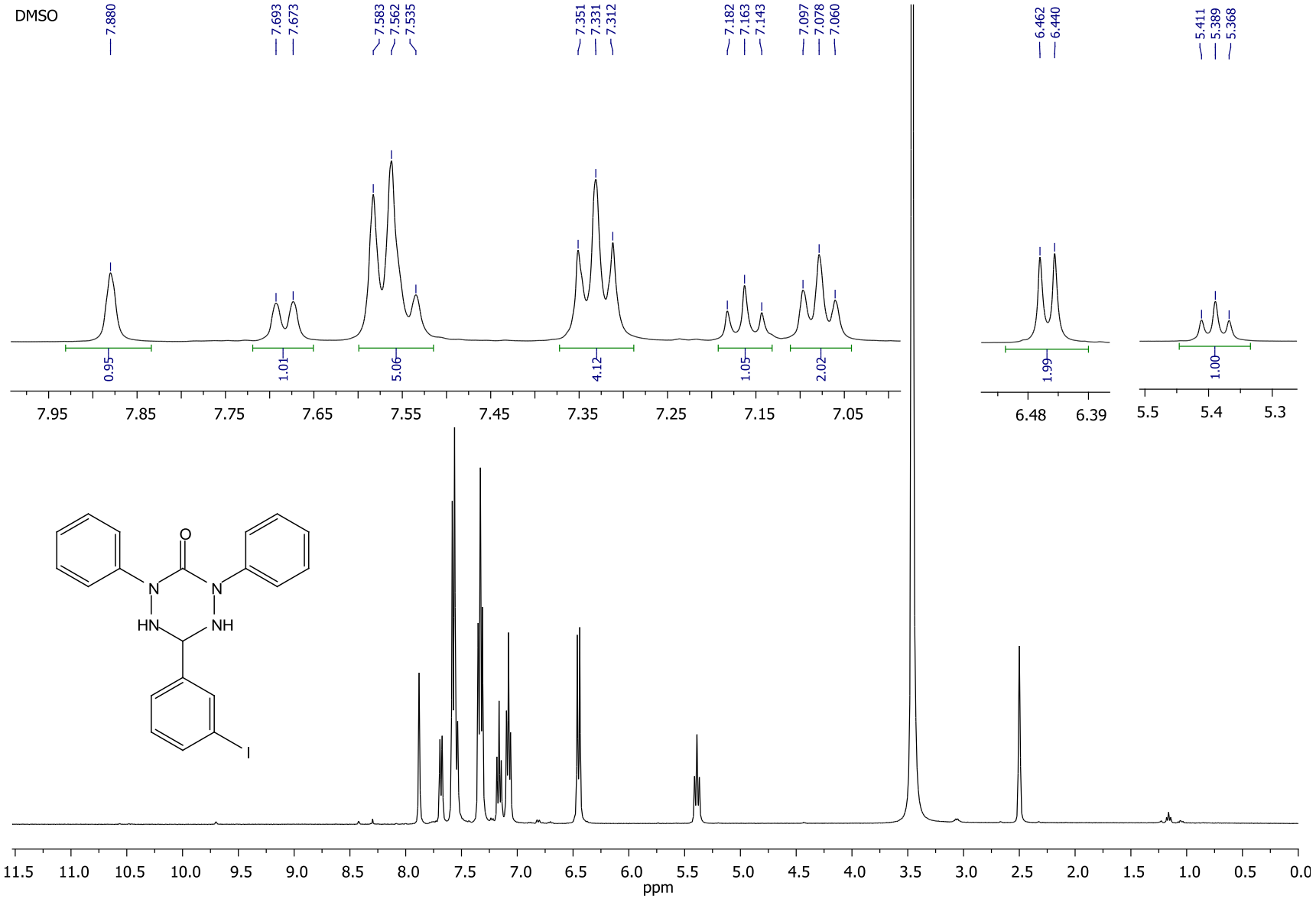


**Fig. S39** $^{1}$H NMR spectrum (DMSO-d6) of 6-(3-iodophenyl)-2,4-diphenyl-1,2,4,5-tetrazinan-3-one **7d.**

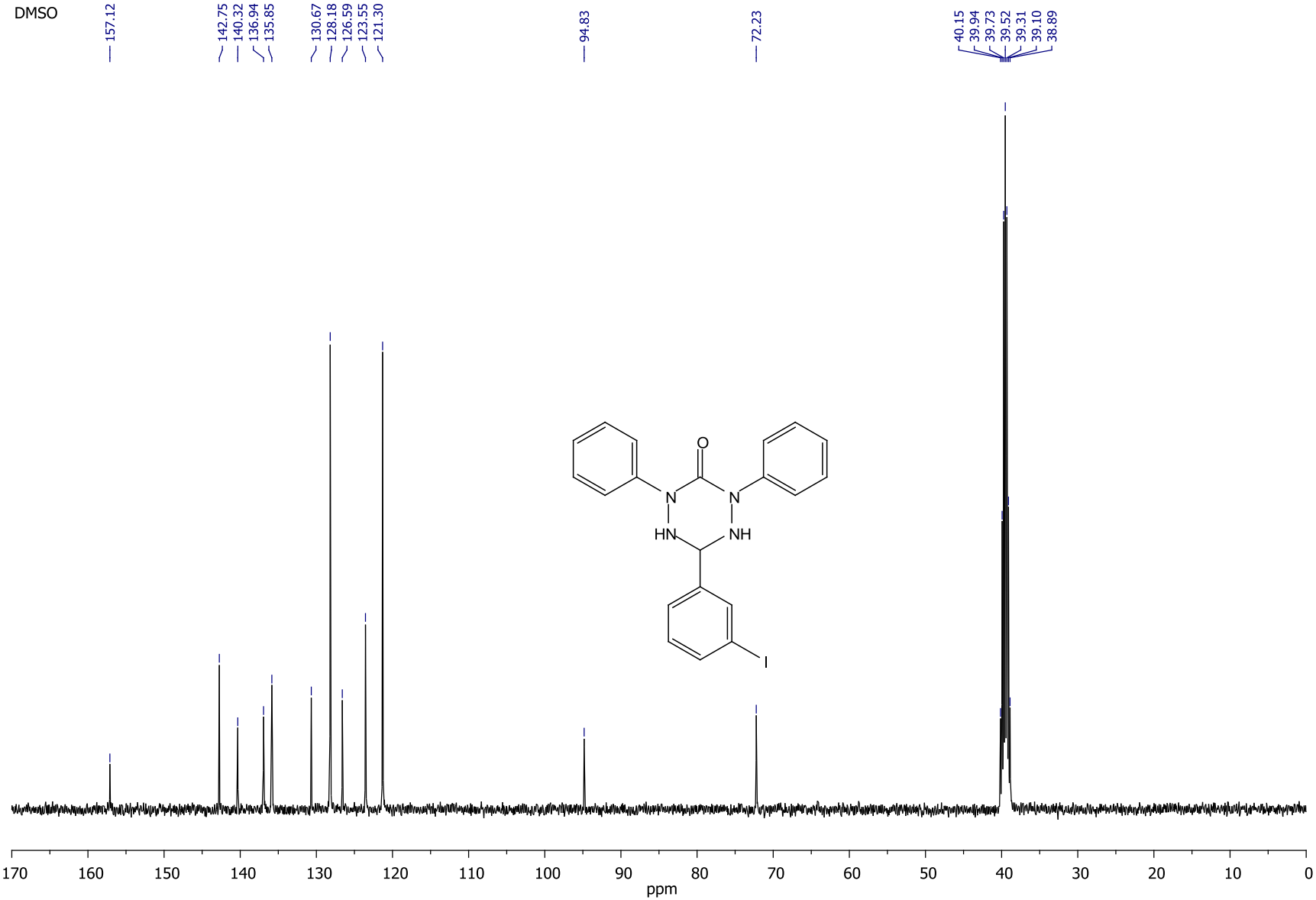


**Fig. S40** $^{13}$C NMR spectrum (DMSO-d6) of 6-(3-iodophenyl)-2,4-diphenyl-1,2,4,5-tetrazinan-3-one **7d.**

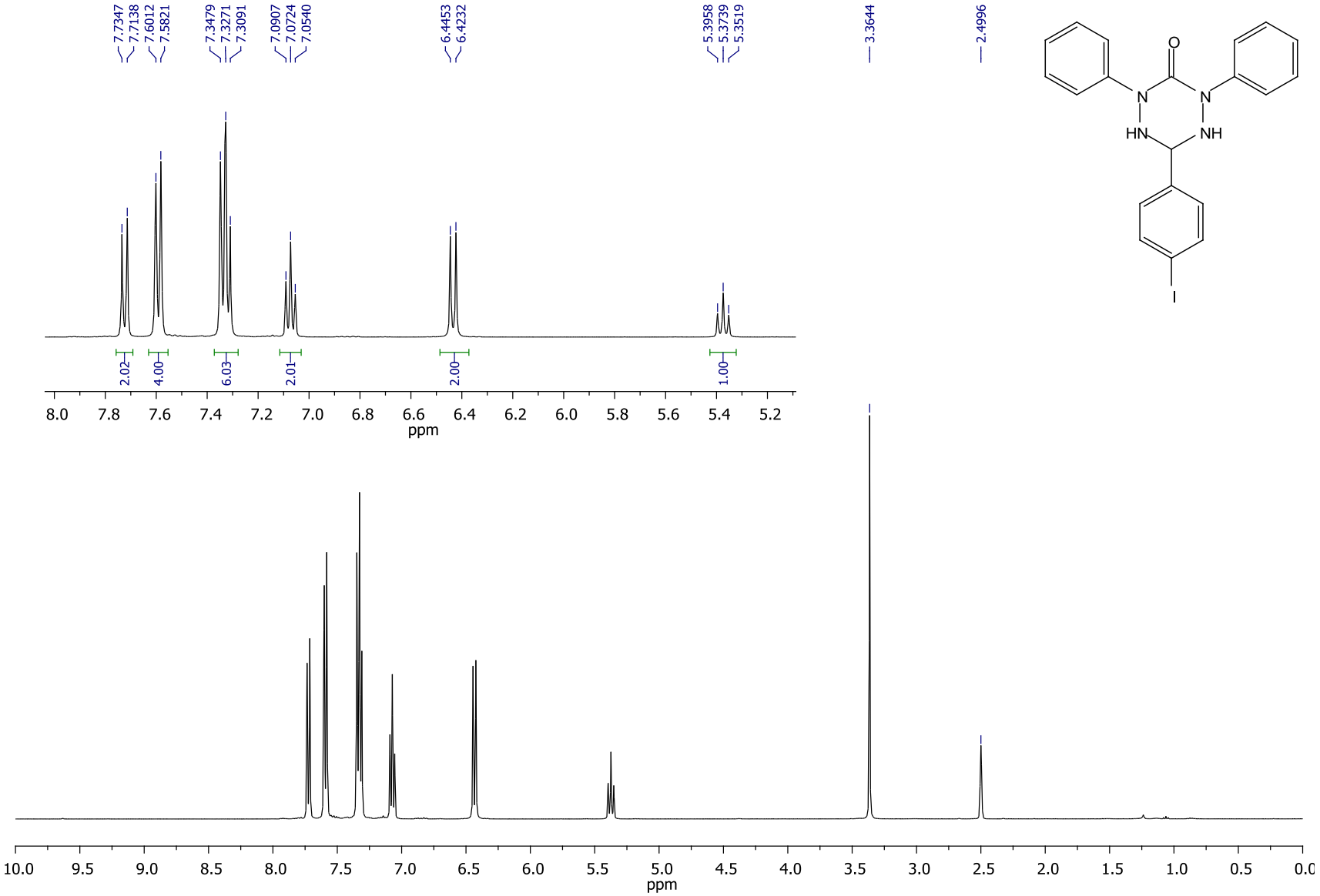


**Fig. S41** $^{1}$H NMR spectrum (DMSO-d6) of 6-(4-iodophenyl)-2,4-diphenyl-1,2,4,5-tetrazinan-3-one **7e.**

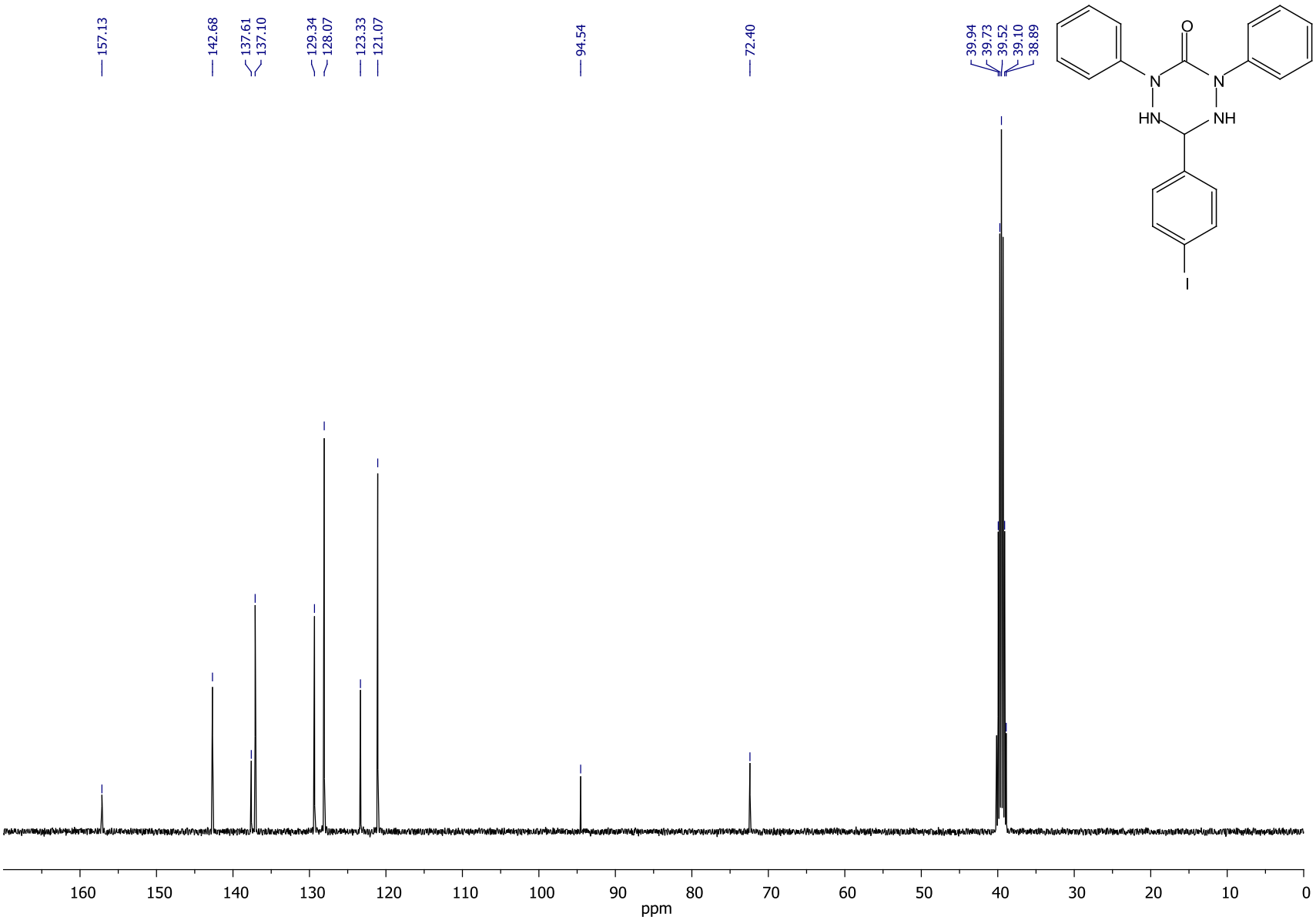


**Fig. S42** $^{13}$C NMR spectrum (DMSO-d6) of 6-(4-iodophenyl)-2,4-diphenyl-1,2,4,5-tetrazinan-3-one **7e.**

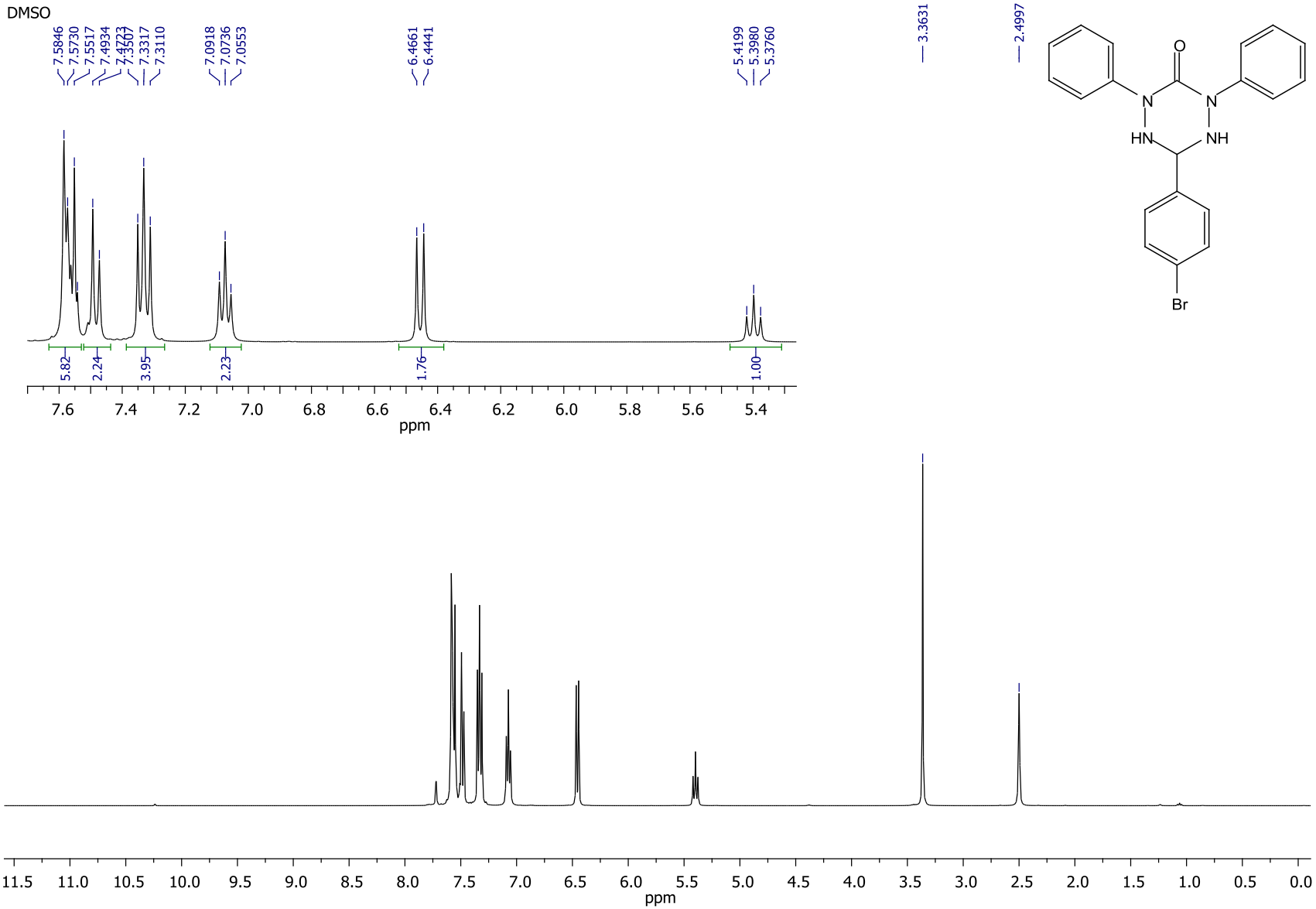


**Fig. S43** $^{1}$H NMR spectrum (DMSO-d6) of 6-(4-bromophenyl)-2,4-diphenyl-1,2,4,5-tetrazinan-3-one **7f.**

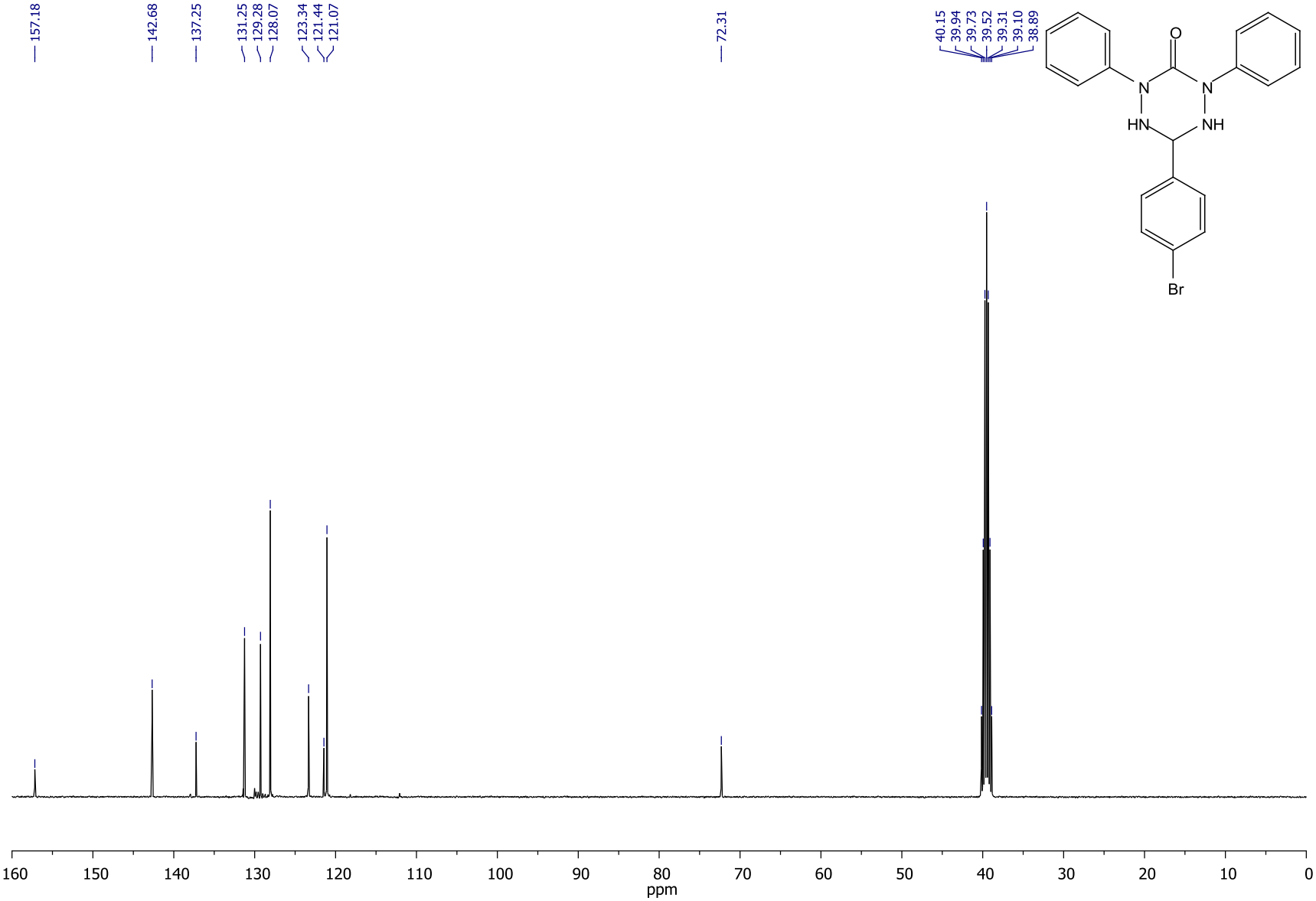


**Fig. S44** $^{13}$C NMR spectrum (DMSO-d6) of 6-(4-bromophenyl)-2,4-diphenyl-1,2,4,5-tetrazinan-3-one **7f**

**References**


1) J. P. Flemming, M. C. Pilon, O. Y. Borbulevitch, M. Y. Antipin and V. V. Grushin, *Inorganica Chim. Acta*, 1998, **280**, 87–98.
2) S. Zhang, Z. Zhang, H. Fu, X. Li, H. Zhan and Y. Cheng, *J. Organomet. Chem.*, 2016, **825–826**, 100–113.